

# The Proportion of Stars with Planets

M. M. Woolfson<sup>1</sup>

Received: 27 September 2015 / Accepted: 2 February 2016 / Published online: 8 February 2016  
© Springer Science+Business Media Dordrecht 2016

**Abstract** Estimates of the proportion of Sun-like stars with accompanying planets vary widely; the best present estimate is that it is about 0.34. The capture theory of planet formation involves an interaction between a condensed star and either a diffuse protostar or a high-density region in a dense embedded cluster. The protostar, or dense region, is tidally stretched into a filament that is gravitationally unstable and breaks up into a string of protoplanetary blobs, which subsequently collapse to form planets, some of which are captured by the star. A computational model, in which the passage of collapsing protostars, with initial radii 1000, 1500 and 2000 au, through a dense embedded cluster are followed, is used to estimate the proportion of protostars that would be disrupted to give planets, in environments with star number-densities in the range  $5000\text{--}25,000\text{ pc}^{-3}$ . It is concluded from the results that the capture theory might explain the presently-estimated proportion of stars with exoplanet companions, although other possible ways of producing exoplanets are not excluded.

**Keywords** Planet formation · Numerical methods · Capture theory

## 1 The Standard Model and Planet Formation

Since the first detection of a planet around the main-sequence star, 51 Pegasus, by Mayor and Queloz (1995), the number of planets detected around stars has increased at an astonishing rate. On 22nd September 2015 the NASA Exoplanet Archive (NASA 2015) listed 1892 confirmed planets, 488 multi-planet systems and 4624 Kepler candidates for transiting exoplanets. When the only planetary system known was the Solar System, a theory could not be discounted on the grounds that it would make planetary formation a

---

✉ M. M. Woolfson  
mmw1@york.ac.uk

<sup>1</sup> Physics Department, University of York, Heslington, York YO10 5DD, UK

rare, or even unique, occurrence. Now a plausible theory must explain planet formation in terms of processes that routinely occur, so making planetary systems common. The proportion of stars with planets is not known, especially as less massive planets are more difficult to detect; estimates, based on observations, are made from time-to-time and generally increase with time. The best current estimate is 0.34 (Borucki et al. 2011) but there are even higher estimates.

The standard model of star and planet formation is that they form by a monistic process. An initial cloud of dusty gas evolves into a central star and a circumstellar disk within which planets form by a multistage process. The dust in the cloud settles into the mean plane of the disk (Weidenschilling et al. 1989) and then, through gravitationally instability, the disk fragments to give planetesimals (Goldreich and Ward 1973), solid bodies with dimensions from hundreds of metres to tens of kilometres. Planetesimals then accumulate over time to give either terrestrial planets or the cores of major planets (Safronov 1972); the latter bodies are assumed to have formed while disk gas is still present, which is then captured to form atmospheres. Observations show that many young stars have a surrounding disk but it has not been possible to quantify the proportion of planetary systems that would form in this way, although the consensus view is that the model would give many planetary systems.

## 2 The Capture Theory and Planet Formation

An alternative theory of planet formation, the capture theory (CT), involves an interaction between a condensed star—either a main-sequence star or YSO—and either a diffuse protostar or a high-density region of gas formed by the collision of turbulent gas streams within a star-forming region. Capture-theory scenarios have been modelled using smoothed-particle hydrodynamics (SPH) and show that the protostars, or high-density regions, can be drawn into dense filaments within which protoplanetary condensations form (Fig. 1; Oxley and Woolfson 2004). The collapse of a condensation over a period of 4000 years is shown in Fig. 2. Some of the protoplanets are captured by the star while others are released into interstellar space and are observed as *free-floating planets* (Lucas and Roche 2000; Sumi et al. 2011). The condensations are typically of gas-giant mass but some are within the brown-dwarf range; in the 2004 paper the planet masses in two simulated interactions, one with a protostar and the other with a high-density region, varied between  $0.75 M_J$  and  $20.5 M_J$ , where  $M_J$  is Jupiter mass. In the Oxley and Woolfson paper the closest approach of star and protostar was 600 au; many simulations have shown that the CT mechanism is extremely robust and has been shown to be valid over a range of scales from one-tenth of that in the Oxley and Woolfson paper to ten times the scale, with appropriate densities and masses of the involved bodies.

The initial orbits of the protoplanets are typically with semi-major axes of order 1000–2000 au and eccentricities in the range 0.9–0.95. However, the CT simulations show that some protostar material is captured in the form of a circumstellar disk, with masses usually in the range 25–50  $M_J$  but sometimes greater. Woolfson (2003) has shown that the disk material acts as a resisting medium within which the protoplanet orbits both decay and round-off. Figure 3 shows the evolution of the orbit of a protoplanet of mass  $1.0 M_J$  in a resisting medium of mass  $25 M_J$  with exponential fall-off of density with distance from the star. Depending on the mass, form and duration of the resisting medium, planets can end up very close to, or very far from, the star, as

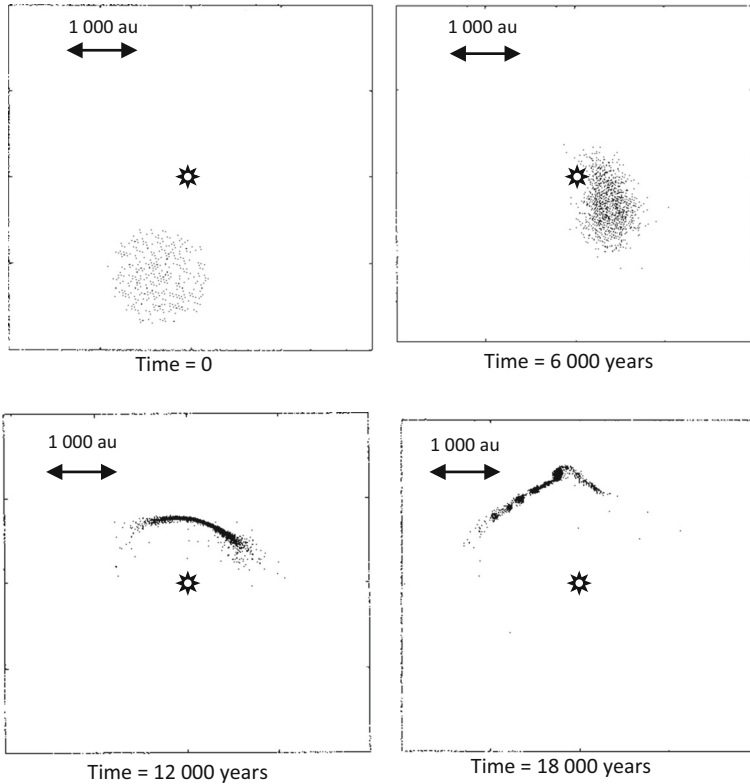
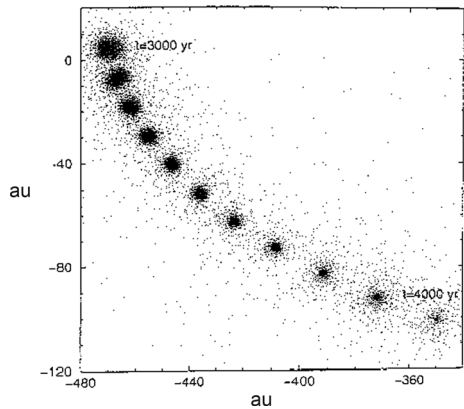


**Fig. 1** An SPH simulation of the interaction of a star and a protostar (Oxley and Woolfson 2004)

**Fig. 2** The collapse of a protoplanet at 100 year intervals (Oxley and Woolfson 2004)



observations have shown. If the star is very active, so applying forces on the medium material, and/or the medium has a toroidal form, orbits of high eccentricity can be the outcome, again in agreement with observations. A medium of toroidal form, given by a CT simulation, is shown in Fig. 4.

While the protoplanets are in extended orbits they are vulnerable to being detached from their stars by stellar perturbation within the dense stellar environment. While many planets

**Fig. 3** The variation with time of **a** semi-major axis and **b** eccentricity (Woolfson 2003)

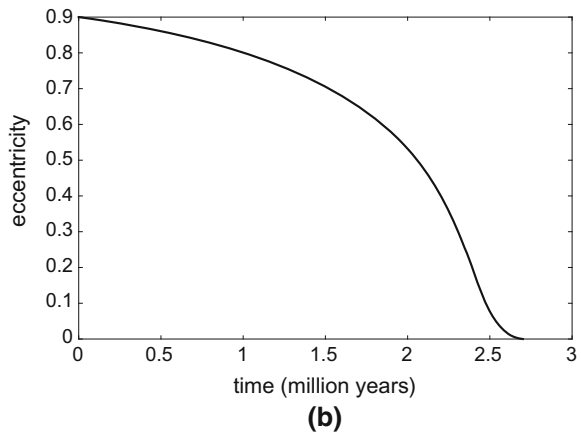
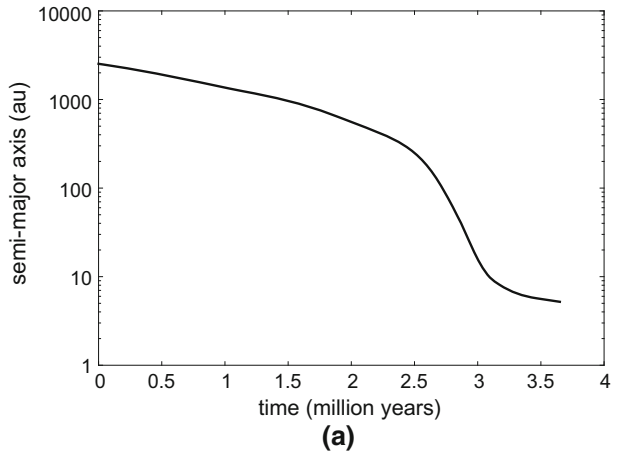
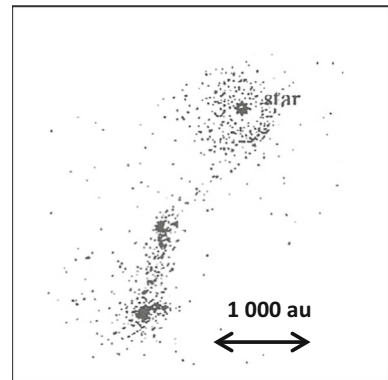


**Fig. 4** A capture-theory simulation showing a strong doughnut-like captured medium. Two condensations, both of brown dwarf mass, are shown (Woolfson 2003)



are removed in this way the number of complete planetary systems removed is small and the proportion of stars with at least one planetary companion is not greatly changed (Woolfson 2004).

The primary CT mechanism can only produce major planets or brown dwarfs; It has been proposed that the larger solar-system terrestrial planets, Earth and Venus, are the residual cores of two erstwhile gas giants that collided in the early Solar System (Woolfson 2013a). This proposal has been shown to be plausible by an SPH simulation (Fig. 5) and the possibility of such an event is supported by a NASA Spitzer Space Telescope observation in August 2009 of the residue of a planetary collision within the last few thousand years in the vicinity of the young star HD172555 (age 12 My). The collision hypothesis also provides explanations for many other features of the Solar System in terms of the destinations of debris from the collision and of ex-satellites of the colliding planets.

The CT produces an almost coplanar system in the plane of the star-protostar orbit and, since there is no relationship between the plane of the star-protostar orbit and the spin axis of the star, it gives a range of spin-orbit misalignments, including retrograde planetary motions. On that basis alone, all spin-orbit misalignments between  $0^\circ$  and  $180^\circ$  would be

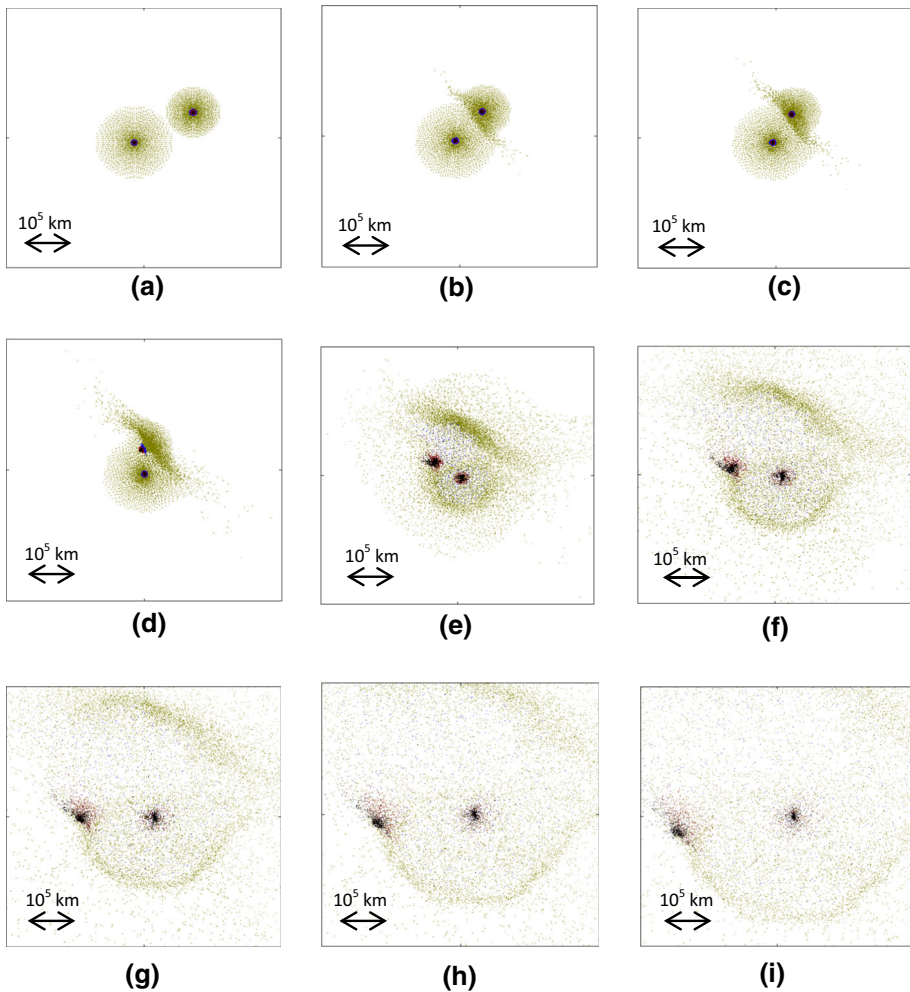


**Fig. 5** The progress of the planetary collision. **a**  $t = 0$ , just before contact, **b**  $t = 501$  s, **c**  $t = 1001$  s, **d**  $t = 1501$  s, **e**  $t = 2003$  s, **f**  $t = 2511$  s, **g**  $t = 3004$  s, **h**  $t = 3502$  s and **i**  $t = 4005$  s (Woolfson 2013a)

equally probable. However, CT simulations show that some CT material impacts the star and is absorbed by it, and other material from the formed disk may also be absorbed. The angular momentum associated with this absorbed material, has the effect of pulling the spin axis of the star towards the normal to the orbital plane of the planets, so reducing the spin-orbit misalignment. Given that the magnitude of the solar angular momentum is equivalent to about one-quarter of a Jupiter mass orbiting at its equator, it will be seen that comparatively small masses of material absorbed by the star can have a large effect in reducing the spin-orbit misalignment. The model gives a complete explanation of the observations that, while the complete range of spin-orbit misalignments is present, there is a strong bias towards smaller values (Woolfson 2013b).

### 3 Dense Embedded Clusters

It is now generally accepted that population I stars like the Sun form in clusters. A collapsing star-forming cloud is gravitationally bound together by the combination of the mass of gas plus that of the growing cluster of stars. In this state, with stars immersed in gas, the cluster is said to be in an *embedded state*. Bonnell et al. (2003) used a high-definition SPH approach to study the evolution of a star-forming cloud. In the final stages of the collapse, lasting about  $5 \times 10^5$  years, the cloud fragments into regions containing up to many tens of stars within which the stellar number-density (SND) can be very high, up to  $2 \times 10^5 \text{ pc}^{-3}$ , although the average SND in the cloud will be two orders of magnitude lower. Thereafter the small fragments combine to form larger fragments, the peak SND in fragments declines but the SND for the cloud as a whole increases. This shows that while fragments are becoming more diffuse they are moving closer together so increasing the whole-cloud SND. In the final stages of the simulation there were 400 stars in five fragments with the maximum fragment SND somewhat greater than  $2 \times 10^4 \text{ pc}^{-3}$  and with whole-cloud SND peaking at  $2 \times 10^4 \text{ pc}^{-3}$ .

One result from the simulation was to show that between 80 and 90 % of stars with masses greater than  $1 M_{\odot}$  have closest approaches to other stars of less than 100 au. The effect of such close stellar interactions in a dense embedded environment was described by Kroupa et al. (1999) who compared the frequency of binary systems in the Taurus–Auriga dark cloud and the Orion Nebula. The frequency of binary systems is significantly lower in the Orion Nebula, which has a much higher SND, and this was interpreted as being due to a greater number of disruptive stellar interactions with binary systems.

The existence of a dense embedded cluster (DEC) has also been invoked to explain the formation of massive stars. The accretion of gas onto a growing core eventually gives a critical mass for which the emitted radiation neutralizes gravitational effects on local gas, preventing further growth. The solution suggested is that in the dense environment at the heart of the forming cluster, smaller mass stars can aggregate to form much more massive stars (Bonnell et al. 1998).

Capture-theory interactions are most likely to occur in a DEC. Although the CT can produce protoplanets by interactions of a star with an amorphous cloud of gas produced by the collision of turbulent gas streams, which may have dimensions of many thousands of au and which may or may not eventually become a protostar, we will restrict our investigation of the frequency of planetary systems to interactions of stars with protostars of initial radii between 1000 and 2000 au. At the end of their 2004 paper, Oxley and Woolfson used an analytical approach to estimate the proportion of stars that would acquire planets in this

way and concluded that it would be more than the 7 % estimate from observations at that time. Here a computational approach will be used, based on experience gained in the last decade from CT simulations.

#### 4 Positioning the Stars in the Model

The basis of this model is to solve the equations of motion for a protostar moving within an environment of fixed SND. A protostar of standard mass  $0.3 M_{\odot}$  has been used with three different radii—1000, 1500 and 2000 au; initial radii some two to three times larger have been suggested by some authors (Phillips 1999). The associated densities give free-fall times of  $t_{ff} = 10,200, 18,800$  and  $28,900$  years, respectively. As the protostar moves among the stars it collapses and its motion is followed for a maximum period  $0.8 t_{ff}$ , at which stage it will have just over one half of its original radius.

The initial configuration of stars is set up in a cell structure, where a cubical cell, containing  $N_S$  stars in randomly-chosen positions, is surrounded by 26 ‘ghost cells’ each containing a similar configuration. When a star moves out of the central cell it re-enters at a similar point on the opposite face, so keeping the density constant. This cell technique is commonly used in studying liquid structure where the liquid has effectively an infinite extent. Lennard–Jones forces, which apply for most normal liquids, are short-range so that molecules outside the neighbouring ghost cells have a negligible effect. In the present application, gravitational forces are not short-range but the region containing the stars, simulating a fragment of a DEC, has a limited extent. The length of the side of the cell,  $a$ , is chosen to give the required stellar number-density and the stars in the ghost cells are only included out to a distance  $ma$  from the centre of the central cell, so giving a spherical cluster containing, on average,  $N_T$  stars where

$$N_T = 4\pi m^3 N_S / 3. \quad (1)$$

We are taking this as the contents of one of the dense fragments in the cloud and we will consider the motion of the protostar as affected by these stars plus the residual gas in the fragment. This mass of gas has two effects—firstly, its gravitational influence on the motion of the stars and protostar and secondly, by exerting a drag on bodies moving within it and so reducing their speeds. Most calculations presented here take the ratio of the mass of gas to that of stars equal to unity. A comparison calculation is also made with the ratio equal to three. The gas mass is taken as uniformly distributed within the dense fragments. Other fragments in the cloud will be sufficiently far from the main fragment for their effect to be in the form of a tidal perturbation and neglecting their influence will not substantially affect the outcome of the calculation.

The drag effect of the gas, and its influence on the speed of bodies moving within it, is discussed in Sect. 7.

#### 5 The Interaction Conditions for Planet Formation

In the development of the CT many calculations were carried out under different conditions to explore the possible range of outcomes. Calculations were made with a variety of star and protostar masses, protostar radii and eccentricities and periastron distances for the star-protostar orbit. For these calculations, admittedly limited in number, interactions for a

solar-mass star in which the periastron of the centre of the protostar was between 0.5 and 1.5 of the radius of the protostar always led to planet formation; these limits are somewhat restrictive since some simulations gave planet formation with ratios outside those limits. It may seem that a periastron less than the protostar radius should lead to a collision, but this does not happen since the protostar is drawn out into the form of a filament. In Fig. 1, the star has solar mass and the ratio of periastron distance to protostar radius is 0.75. Using the relationship that tidal effects due to a body of mass  $M$  at a distance  $d$  varies as  $M/d^3$  we use as the range of distance,  $r_c$ , for a CT interaction as

$$0.5 \left( \frac{M_{\odot}}{M_*} \right)^{1/3} R_p \leq r_c \leq 1.5 \left( \frac{M_{\odot}}{M_*} \right)^{1/3} R_p \quad (2)$$

where  $M_*$  is the star mass and  $R_p$  is the current radius of the collapsing protostar. This range is not theoretically correct because the  $1/d^3$  relationship is true only for distances much larger than the radius of the body being tidally affected, but it gives the right general form for dependence on stellar mass.

When the initial position of the protostar is fixed it is checked to see that it is more than two of its radii distant from the nearest star. This is based on the idea that a protostar could not form too near an existing condensed star. However, this is another conservative condition since, as previously mentioned, Oxley and Woolfson (2004) showed that an interaction between a condensed star and a high density region in the star-forming cloud, formed by the collision of gaseous turbulent elements, can also lead to planet formation without the need for the condensed region first to form a protostar, and such collisions can occur close to stars.

## 6 The Masses of the Stars

As a galactic cluster collapses in the embedded stage the mean density,  $\rho$ , of the gas increases as does the turbulence. Increases in temperature,  $T$ , are moderated by radiation processes so the Jeans critical mass for the gas, which varies as  $(T^3/\rho)^{1/2}$ . Reduces with time. This is reflected in the way that the average mass of the stars produced, initially about  $1.2 M_{\odot}$ , reduces with time (Williams and Cremin 1969; Woolfson 1979); some later-produced stars are of mass higher than  $M_{\odot}$ , but this is consistent with the idea of the amalgamations of stars produced earlier by the primary star-forming process (Bonnell et al. 1998). Most of the stars in a DEC would have formed at an earlier stage and hence will mostly be more massive than the protostars being formed. For this reason the masses of the stars are chosen by random selection from a distribution with mass index  $\sim 2.3$  (Kroupa 2001) i.e.

$$f(M) \propto M^{-2.3}, \quad (3)$$

with masses in the range  $0.5\text{--}3.0 M_{\odot}$ , all greater than the mass of the protostar. For each star a uniform deviate,  $s$ , in the range  $0\text{--}1$ , is generated and then the mass of the star in solar units is given by

$$M = \{0.5^{-1.3} + s(3^{-1.3} - 0.5^{-1.3})\}^{-\frac{1}{1.3}}, \quad (4)$$

which gives the correct distribution.



The average mass of the stars so generated, in solar units, is given by

$$M_{av} = \frac{\int_{0.5}^3 Mf(M)dM}{\int_{0.5}^3 f(M)dM} = \frac{\int_{0.5}^3 M^{-1.3}dM}{\int_{0.5}^3 M^{-2.3}dM} = 1.00 \tag{5}$$

### 7 The Speeds of Stars

The speeds of the stars, and particularly the speed of the protostar, affect the probability of a CT interaction in two contradictory ways. The greater is the speed of the protostar the greater the distance it will travel in the DEC and the more likely it is to come close to a star. On the other hand, the slower the relative protostar-star speed the greater will be the gravitational interaction cross-section, so the more likely it is that on approaching a star the protostar will be deflected into a position to become tidally distorted and disrupted. In Fig. 6 the line of approach of a body of mass  $M_p$  to another of mass  $M_*$  is shown with the relative speed at a large distance  $V$ , as shown in the figure, and a closest approach  $r$ . The gravitational cross-section for this closest approach is

$$\pi D^2 = \pi r \left( r + \frac{2G(M_* + M_p)}{V^2} \right). \tag{6}$$

To give an idea of the relative importance of the two terms in parentheses we take

$$M_* + M_p = M_{\odot}, V = 1 \text{ km s}^{-1} \quad \text{and} \quad r = 600 \text{ au}.$$

This gives the gravitational cross section of  $1.01 \times 10^{29} \text{ m}^2$  as against a geometrical cross-section  $\pi r^2$  (gravity not acting, i.e.  $G = 0$ ) of  $2.54 \times 10^{28} \text{ m}^2$ , i.e. almost four times higher. For a CT interaction to take place the effective gravitational cross section is the difference of two terms as given by (6) with the values of  $r$  given by the limits indicated in (2).

We must now consider the speeds to assign to the stars in the model DEC. For a collection of gravitationally interacting stars in a bound region in equilibrium, and with no

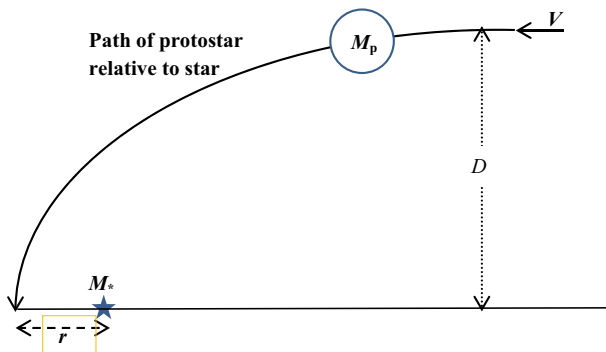


Fig. 6 Path of a protostar to give closest approach distance  $r$

other forces acting, the virial theorem would be valid. This gives the kinetic energy,  $K$ , of the motions of the stars related to their total potential energy,  $\Omega$ , by

$$K = -0.5\Omega \tag{7}$$

However, due to the action of gas dynamical friction, the stars in a DEC will have sub-virial energy (Indulekha 2013) so that

$$K = -\alpha\Omega \tag{8}$$

with  $\alpha < 0.5$ . Following a similar theme Proszkov et al. (2009) have considered  $\alpha$  in the range 0.04–0.15. This range of  $\alpha$  corresponds to root-mean-square speeds between 28 and 55 % of the virial value.

The next decision is how to allocate the kinetic energy to the stars—one possibility is to give stars a speed selected from the same distribution regardless of their mass and another is to take all stars with the same expectation energy, i.e. to invoke the equipartition-of-energy principle. The latter alternative was chosen with stars, and the protostar, given speeds corresponding to the equipartition value in a randomly-chosen direction. Thus with  $N_T$  stars in the cluster the  $i$ th star has a speed

$$V_i = \left( -\frac{2\alpha\Omega}{N_T M_i} \right)^{1/2} \tag{9}$$

We can estimate the speeds assigned to stars of the extreme masses,  $0.5 M_\odot$  and  $3.0 M_\odot$  as a function of the SND. The radius of the cluster is

$$r_{CL} = ma = m \left( \frac{N_S}{n} \right)^{1/3} \text{ pc} = m \left( \frac{N_S}{n} \right)^{1/3} \times 3.09 \times 10^{16} \text{ m}$$

where  $n$  is the star number density in  $\text{pc}^{-3}$ . For the  $N_T$  stars in the cluster, with average mass  $M_{av}$ , the potential energy is closely equal to that of the total mass of the stars uniformly distributed within a sphere of radius  $r_{CL}$  which is, with all quantities in SI units,

$$\Omega = -\frac{3G(N_T M_{av})^2}{5 r_{CL}} = -\frac{3G(N_T M_{av})^2}{5 m} \left( \frac{n}{N_S} \right)^{1/3} \frac{1}{3.09 \times 10^{16}} \text{ J} \tag{10}$$

As an example we take  $N_S = 23$ ,  $m = 1.0$ , giving  $N_T = 96$  and  $M_{av} = M_\odot$ , which gives

$$\Omega = -1.65 \times 10^{37} n^{1/3} \text{ J}$$

For  $\alpha = 0.04$  and with the kinetic energy shared equally by the  $N_T$  stars, each star has energy

$$E_* = -0.04\Omega/N_T = 6.88 \times 10^{33} n^{1/3} \text{ J}$$

and the  $i$ th star has speed

$$V_i = \left( \frac{2E_*}{M_i} \right)^{1/2} = 1.17 \times 10^{17} \left( \frac{n^{1/3}}{M_i} \right)^{1/2} \tag{11}$$

For  $n = 5000 \text{ pc}^{-3}$  and  $M_i = 0.5 M_\odot$   $V_i = 483 \text{ m s}^{-1}$ .

For  $n = 5000 \text{ pc}^{-3}$  and  $M_i = 3.0 M_\odot$   $V_i = 198 \text{ m s}^{-1}$ .

For  $n = 25,000 \text{ pc}^{-3}$  and  $M_i = 0.5 M_\odot$   $V_i = 632 \text{ m s}^{-1}$ .

For  $n = 25,000 \text{ pc}^{-3}$  and  $M_i = 3.0 M_\odot$   $V_i = 258 \text{ m s}^{-1}$ .

For comparison, Gaidos (1995) gave stellar speeds in a DEC in the range 500–2000  $\text{m s}^{-1}$ , corresponding to a larger value of  $\alpha$  and allowing larger values of  $n$ .

## 8 The Computational Algorithm

With the SND fixed and the positions and velocities of the stars and protostar set, the equations of motion are numerically solved for the  $N_S$  stars plus protostar in the basic cell. The gravitational effects of the stars in the ghost cells are taken into account but they are not moved during the integration step. The gravitational acceleration due to the gas, of mass  $M_T$ , within the fragment on a star at vector position  $\mathbf{r}$  was included and is given by

$$\mathbf{a}_r = \frac{GM_T}{(ma)^3} \mathbf{r} \quad (12)$$

The basic integration is carried out using the 4-step Runge–Kutta method; keeping the stars in the ghost cells unmoved is equivalent to what happens in the simple Euler method and is acceptable if the motions of the stars are not too large at each integration step. The initial timestep,  $h$ , was set at  $10^6$  s and the motions were advanced separately in two calculations, one using two timesteps of  $h$  and another with one timestep of  $2h$ . If for these two calculations the positions of every star agreed to within  $10^8$  m (0.00067 au) and the magnitude of every velocity difference was less than  $10 \text{ m s}^{-1}$  then the step was accepted and the positions and velocities were advanced to the values given by the two steps of  $h$ . Then the timestep was increased to  $2h$  and the calculation was continued. However, if the tolerance conditions were not met then the step was repeated with a halved timestep, i.e. back to  $h$ . Timesteps are repeatedly halved until the tolerance conditions are met. The timesteps throughout the whole calculation were generally between  $1.6 \times 10^7$  and  $2.56 \times 10^8$  s, mostly at the upper end of that range. If the motion of the protostar gives a periastron distance from a star between 0.5 and 1.5 of its current radius (which changes with time) then planet formation is deemed to have occurred but if it moves closer than 0.5 times its radius then it is taken that the protostar is disrupted without planet formation. If the planet formation or protoplanet disruption stage is reached then the trial is terminated and the next one begun, otherwise the calculation is terminated at time  $0.8 t_{ff}$ .

At the end of each integration step any stars, including the protostar, that have left the basic cell are reintroduced into the cell as described in Sect. 4, the ghost cells are set up from the revised basic cell and the cluster then redefined as the stellar contents within distance  $ma$  of the centre of the basic cell.

## 9 Results

Trials were run with the three protostar radii—1000, 1500 and 2000 au—and with stellar number densities  $n = 5000, 10,000, 15,000, 20,000$  and  $25,000 \text{ pc}^{-3}$ . The first trials were to test the effect of different degrees of sub-virial speeds, taking  $\alpha = 0.04, 0.10$  and  $0.50$ . For each  $\alpha$ , 1000 trials were run with  $n = 15,000 \text{ pc}^{-3}$ ,  $R_p = 1000, 1500$  and  $2000$  au,  $N_S = 23$  and  $m = 1.0$ , corresponding to  $N_T = 96$ . The results, in terms of percentages, are shown in Table 1, where N corresponds to ‘no capture’, C indicates ‘capture’ and T indicates ‘too close’.

**Table 1** Variation of outcomes for different values of  $\alpha$ 

$n$	$R_p$ (au)	$\alpha = 0.04$			$\alpha = 0.10$			$\alpha = 0.50$		
		N	C	T	N	C	T	N	C	T
15,000	1000	94.9	2.1	3.0	97.0	1.9	1.1	96.5	3.2	0.3
15,000	1500	84.5	8.9	6.6	87.5	9.3	3.2	83.5	13.2	3.3
15,000	2000	69.6	25.9	14.5	62.2	27.8	10.0	41.0	49.4	9.6

The indication from Table 1 is that the higher the value of  $\alpha$  the higher is the probability of capture so exploring the behaviour of the model with  $\alpha = 0.04$  should not be exaggerating the effectiveness of the CT mechanism. Now a fuller set of results, for the full ranges of  $n$  and  $R_p$  with  $\alpha = 0.04$  is given in Table 2, where only the percentage of capture events in 1000 trials is given. They are carried out with  $N_S = 8$  and  $m + 1.5$ , giving  $N_T = 113$  (set A),  $N_S = 23$ ,  $m = 1$ , giving  $N_T = 96$  (set B), which was used for Table 1, and  $N_S = 10$ ,  $m = 1$ , giving  $N_T = 42$  (set C). In all these cases the ratio of gas mass to stellar mass is one.

The results for the three sets are quite similar, the differences being within the bounds of what would be expected in a Monte-Carlo type calculation. The results of the calculations are shown graphically for the average of sets A, B and C in Fig. 7 with smooth Bézier curves representing the variation of the capture percentage, which eliminates the fluctuations of the Monte Carlo process with a relatively small number of trials.

The additional column, marked D, is for the conditions of set C but with the ratio of gas mass to star mas equal to three. The proportion of capture events is of the same order as for set C although tending to be somewhat higher for high stellar densities and larger protostar

**Table 2** Percentage of CT interactions with various  $R_p$  and  $n$ 

$R_p$ (au)	$n$	Set A capture (%)	Set B capture (%)	Set C capture (%)	Average capture (%)	Set D capture (%)
1000	5000	0.7	0.6	0.3	0.5	0.3
	10,000	1.8	1.6	1.0	1.5	0.8
	15,000	3.4	2.1	1.8	2.4	1.9
	20,000	3.8	3.3	2.9	3.3	3.2
	25,000	5.3	4.5	4.6	4.8	5.3
1500	5000	2.3	2.3	2.7	2.4	2.4
	10,000	6.5	5.6	5.9	6.0	5.5
	15,000	11.6	8.9	10.2	10.2	11.0
	20,000	11.5	13.5	11.9	12.3	12.9
	25,000	15.9	16.3	17.1	16.4	19.5
2000	5000	7.9	6.6	5.0	6.5	5.2
	10,000	17.7	16.9	16.7	17.1	17.0
	15,000	29.0	25.9	24.7	26.5	29.1
	20,000	36.4	37.8	33.6	35.9	40.8
	25,000	48.0	46.0	44.2	46.1	52.4

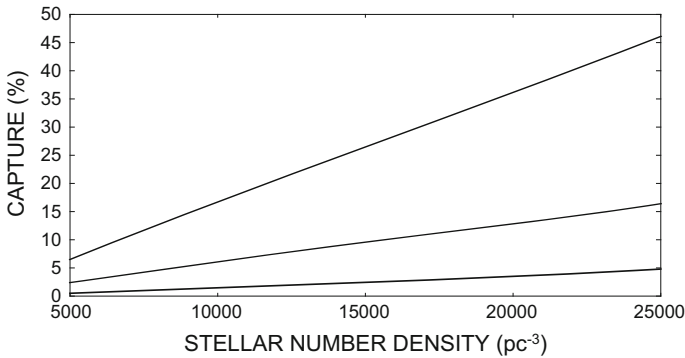


**Fig. 7** Proportion of stars with planets for different protoplanet radii ( $R_p$ ) and stellar number densities

radii. These results indicate that taking the ratio of gas mass to star mass equal to unity, the lowest reasonable value, is not exaggerating the proportion of capture events.

### 10 The Proportion of Stars with Planets

What these results show is the proportion of *protostars that form planets* within the different environments. However, what is of interest is the proportion of *stars that acquire planetary systems*. Every star begins its existence as a protostar but the first protostars produced will be in an environment of very small SND and so with a very small probability of producing a capture event. However, later-produced protostars will be in an environment of higher SND and hence, as shown in Table 2, can have a significant probability of producing a capture event. From the work of Williams and Cremin (1969) lower mass stars, and hence protostars, are mostly produced at the end of the star-forming process and this will be when the rate of star formation is high and when both the density of gas is high—giving a smaller Jeans critical mass—and the SNDs are large.

Kroupa (2001) gave the mass index  $-2.3$  in Eq. (3) for stars of mass greater than  $0.5 M_\odot$  but  $-1.3$  for the mass range  $0.08-0.5 M_\odot$ . We first find  $S$ , the ratio of the number of stars produced with masses between  $0.08$  and  $0.5 M_\odot$  to those with masses greater than  $0.5 M_\odot$ . Taking the two distributions as  $A m^{-1.3}$  and  $B m^{-2.3}$ , with  $m$  in solar-mass units, and imposing the condition that these must be the same for  $m = 0.5$ , we find  $A = 2B$ . Hence

$$S = \frac{2 \int_{0.08}^{0.5} m^{-1.3} dm}{\int_{0.5}^{\infty} m^{-2.3} dm} = 3.2. \tag{13}$$

On the simple, but untenable, assumption that all stars of mass greater than  $0.5 M_\odot$  were produced and became compact earlier than the formation of all protostars of mass less than  $0.5 M_\odot$ , then if the proportion of protoplanets producing planets was  $p$  then, at least for small  $p$ , the proportion of stars with planets would be  $p_S = 3.2p$ ; for some of the values of  $p$  in Table 2 the value of  $p_S$  would be greater than 1. Given the distinct trend for larger mass stars to be produced earlier than smaller mass stars, it seems reasonable to take the probabilities in Table 2 as close to  $p_S$ , the probabilities that stars acquire planetary systems.

Embedded clusters have different characteristics, in particular relating to the peak stellar number densities that occur in them, which will depend, amongst other things, on when massive stars evolve to the supernova stage. Some peak densities may be comparatively low, say  $10^3 \text{ pc}^{-3}$ , while others may be several times  $10^4 \text{ pc}^{-3}$  as in the Trapezium Cluster, or even much higher—up to  $10^6 \text{ pc}^{-3}$  according to some authors (McCaughrean and Stauffer 1994; Bonnell and Bate 2005; Adams et al. 2006). The proportion of stars with accompanying planets cannot be estimated directly from the results obtained here since the distribution of peak stellar-number densities in embedded clusters is not known.

As mentioned in Sect. 2, the initial orbits of protoplanets are very extended and, in such an orbit in a high SND environment, there is a possibility that, before its orbit has completely evolved, a planet can be perturbed sufficiently to escape from its star. The environment that is conducive to forming planetary systems is also conducive to breaking them up. This question was addressed by Woolfson (2004). Although between one-third and two-thirds of planets may be removed in this way—so adding to the numbers of free-floating planets—since many-planet systems are common, the number of stars left with one or more planets was estimated to be more than 80 % of those initially formed. This result does not substantially affect the estimate of the proportion of stars with planetary systems.

## 11 Conclusions

The plausibility of the postulate that the CT model can explain a substantial proportion of stars with accompanying planets depends on the following conditions being met:

1. DEC's should occur with fragments having large SNDs.
2. Protostars and high-density regions should form in these dense environments.
3. The CT mechanism, as shown simulated in Fig. 1, should be valid.
4. The computational model described in Sect. 8 should, at least, give results of the right order.

Given that the four conditions hold, it seems likely that at least some exoplanets will have formed by the CT mechanism and the analysis, if valid, indicates that the predicted proportion of stars with accompanying planets could be consistent with present estimates.

It should be noted that a number of restrictive conditions have been imposed on the analysis we have used. These are:

5. Capture-theory events involving high-density regions have not been included in the estimate of the proportion of stars with planets.
6. The SNDs have been considered up to  $2 \times 10^4 \text{ pc}^{-3}$ , a value for which there is observational evidence, e.g. in the Trapezium Cluster. Values up to  $10^6 \text{ pc}^{-3}$ , taken by some authors would result in a large proportion of stars having planetary companions.
7. The maximum radius of a protostar has been taken as 2000 au; other authors have suggested much larger values, which again would greatly increase the estimates of the proportion of stars with exoplanetary companions.
8. The value taken for  $\alpha$ , 0.04, gives root-mean-square speeds less than those indicated by Gaidos (1995). Increasing the value of  $\alpha$  would give a higher estimate of  $p_s$ .

In view of the conservative assumptions that have been made with respect to  $R_p$ ,  $n$  and  $\alpha$ , and the exclusion of considering high-density regions as potential planetary sources (which could exceed the number of protostars) the model could accommodate even higher

estimates of the proportion of stars with planets, should the observational evidence so indicate. Taking values for some parameters that have been suggested either by observations or by some authors, it could even be concluded that the majority of stars have planetary companions. For example, with  $R_p = 2000$  au,  $n = 10^5$  pc $^{-3}$  and  $\alpha = 0.04$ , 75.5 % of stars would have planets. However, even with extremely favourable conditions there could never be an estimate of *all* stars with planets. Although every star might have an interaction, some proportion of them would be too close. Even although the results indicate that many exoplanets should form via the CT mechanism, it cannot be claimed that it is the only way for planets to form. In different environments other mechanisms may also operate.

**Acknowledgments** I express my gratitude to a reviewer of this paper for suggestions leading to a better presentation of the work.

## References

- F.C. Adams, E.-M. Proszkov, M. Faluzzo, P.C. Myers, *Astrophys. J.* **641**, 504 (2006)  
I.A. Bonnell, M.R. Bate, H. Zinnecker, *MNRAS* **298**, 93 (1998)  
I.A. Bonnell, M.R. Bate, S.G. Vine, *MNRAS* **343**, 413 (2003)  
I.A. Bonnell, M.R. Bate, *MNRAS* **382**, 915 (2005)  
N.J. Borucki et al., *Astrophys. J.* **736**, 19 (2011)  
E.J. Gaidos, *Icarus* **114**, 258 (1995)  
P. Goldreich, W.R. Ward, *Astrophys. J.* **183**, 1051 (1973)  
H. Indulekha, *J. Astrophys. Astron.* **34**, 207 (2013)  
P. Kroupa, M.G. Petr, M.J. McCaughrean, *New Astron.* **4**(7), 495 (1999)  
P. Kroupa, *MNRAS* **322**, 231 (2001)  
P. Lucas, P. Roche, *MNRAS* **314**, 858 (2000)  
M. Mayor, D. Queloz, *Nature* **378**, 355 (1995)  
M.J. McCaughrean, J. Stauffer, *Astrophys. J.* **108**, 1382 (1994)  
NASA (2015) [exoplanetarchive.ipac.caltech.edu](http://exoplanetarchive.ipac.caltech.edu)  
S. Oxley, M.M. Woolfson, *MNRAS* **348**, 1135 (2004)  
A.C. Phillips, *The physics of stars. Manchester physics series*, 2nd edn. (Wiley, Hoboken, 1999)  
E.-M. Proszkov, F.C. Adama, L.W. Hartmann, J.J. Tobin, *Astrophys. J.* **697**, 1020 (2009)  
V.S. Safronov, *Evolution of the protoplanetary cloud and formation of the earth and planets* (Israel Program for Scientific Translation, Jerusalem, 1972)  
Y. Sumi et al., *Nature* **473**, 349 (2011)  
S.J. Weidenschilling, B. Donn, P. Meakin, in *The formation and evolution of planetary systems*, ed. by H.A. Weaver, L. Danley (Cambridge University Press, Cambridge, 1989), pp. 131–150  
I.P. Williams, A.W. Cremin, *MNRAS* **144**, 259 (1969)  
M.M. Woolfson, *Philos. Trans. R. Soc. Lond.* **A291**, 219 (1979)  
M.M. Woolfson, *MNRAS* **340**, 42 (2003)  
M.M. Woolfson, *MNRAS* **348**, 1150 (2004)  
M.M. Woolfson, *Earth Moon Planet.* **111**, 1 (2013a)  
M.M. Woolfson, *MNRAS* **436**, 1492 (2013b)